MJFAS
Malaysian Journal of Fundamental and Applied Sciences

Baktehir *et al.* | Malaysian Journal of Fundamental and Applied Sciences, Vol. 19 (2023) 202-214

RESEARCH ARTICLE

Blend of Multi-Walled Carbon Nanotubes and Quercetin Improves Physicochemical Properties of Chitosan Membrane for Wound Dressing Application

Nurul Huda Baktehir[a], Mohamad Ajma'in Mohamed Arbi[a], Thiviya Selvaras[a], Norjihada Izzah Ismail[a,b*]

[a]School of Biomedical Engineering and Health Sciences, Faculty of Engineering, Universiti Teknologi Malaysia, 81310 UTM Johor Bahru, Johor, Malaysia; [b]Medical Devices and Technology Centre, Institute of Human Centered Engineering, Universiti Teknologi Malaysia, 81310 UTM Johor Bahru, Johor, Malaysia

Abstract Although wound dressings are essential to protect wound from infection, these wound care products have limited function in facilitating wound healing. This study aimed to synthesize multi-walled carbon nanotube (MWCNT)/quercetin (QUE)/chitosan (CS) blended composite membrane and analyze their physicochemical properties for wound dressing application in comparison to the pure chitosan (CS) membrane. The MWCNT/QUE/CS blended membranes were prepared by mixing CS, QUE and MWCNT at a ratio of 3:1:1 using a solvent casting method. The membranes were analyzed physicochemically for their surface morphology, elemental composition, structural composition, wettability, water vapor transmission rate (WVTR) and swelling properties and were compared to the pure CS membrane. The findings pointed out that the blend of MWCNTs and QUE in the CS matrix produces a membrane with uneven and more hydrophilic surface with water contact angle of 64.70°± 3.7 and low WVTR of 16.26 g/m^2.day after 24 h. The swelling analysis showed that the blended membrane was able to absorb more than 60% of water within 10 minutes, although lower than the pure CS membrane. This study revealed that MWCNT/QUE/CS blended membrane could possibly be used as a wound dressing as it may promote moist environment needed for wound healing in addition to its antibacterial and antioxidant properties that may accelerate wound healing process.

Keywords: Wound dressing, bioactive materials, chitosan biopolymer, quercetin, multi-walled carbon nanotubes.

***For correspondence:**
norjihada@utm.my

Received: 24 Oct. 2022
Accepted: 12 Feb. 2023

Introduction

While skin as the largest organ of the body offers protection, wounds resulted in disintegration of such defensive function of the skin [1]. Wounds which are unable to heal completely after 30 days of treatment with excessive, prolonged inflammation and delayed re-epithelialization are categorized as chronic wounds [2-3]. The failure to resolve the inflammatory phase is contributed by multifactorial stimuli including excessive amounts of pro-inflammatory macrophages, unreasonably high inflammatory mediators such as tumor necrosis factor alpha (TNF-α) and interleukin-1β (IL-1β), release of a number of matrix metalloproteinases (MMPs) by chronic wound macrophages, and limited capability the chronic wound macrophages have to eliminate apoptotic neutrophils. This condition prevents commencement of the subsequent proliferative stage of healing [4-5]. Another issue with wound chronicity is the formation of biofilm infection that protects pathogenic polymicrobes from antimicrobial action and host immune response [4-6]. Interaction of the biofilms with the host

10.11113/mjfas.v19n2.2776

immune system promotes ongoing inflammation [5]. The cationic exopolysaccharide matrix of the biofilms mediate antimicrobial resistance following genetic exchange between bacteria and serves as a protective barrier that prevents immune recognition and elimination by the host immune system [5, 7]. The production and adherence of the biofilms containing polysaccharides such as poly-β-1,6-N-acetylglucosamine (PNAG) and pellicle (Pel) on the cell wall of the bacteria resulted in a wide-range protection including avoid killing by neutrophils and leukocyte-like cell line as well as inhibit complement deposition [7-8].

Since ancient times, dressing has played an important role in wound care and management. It is specifically designed to be in contact with the wound. In fact, types of dressing have evolved from non-occlusive to occlusive with modern dressings arrival in 20th century focusing on facilitating wound function rather than just as a covering [1]. Gauze dressings are one of the most widely used traditional dressings. These dressings are made out of woven and non-woven cotton fibers, viscose and polyesters and are known to provide protection from bacterial infection as well as able to absorb exudates and fluids when used in large quantities. However, gauze dressings require frequent replacement and induce pain during removal due to their adherent to the wound [1-9]. Modern dressings such as hydrogels, hydrocolloids, semi-permeable films, and foams were introduced to promote better wound healing [9]. A comparison study between gauze and silicone dressings revealed that petrolatum gauze dressing gives less patient satisfaction due to its different pattern and intolerable severity of pain [10].

As the biopolymer with good biocompatibility, biodegradability, non-toxicity and antimicrobial activity, chitosan (CS) is widely investigated as a wound dressing material [6]. A recent study revealed that CS fiber dressings absorb blood more effectively and exert hemostatic effects by reducing antithrombin levels and prolonging activated partial thromboplastin time (aPTT) in comparison to the gauze dressing [11]. In another study, a chitosan derivative, *O*-carboxymethylated chitosan was proposed as a suitable anti-inflammatory and analgesic agent following tests in albino rats [12]. On top of that, the addition of natural bioactive secondary metabolites to the wound dressings may potentially promote wound healing. This is due to the numerous features of these compounds such as antioxidant, antibacterial, antifungal and anti-inflammatory which are beneficial for wound healing processes. Studies have shown that the inclusion of essential oils, plant metabolites and extracts in chitosan wound dressing systems provide antimicrobial effects against common wound pathogens such as *Staphylococcus aureus* and *Escherichia coli* [6, 13]. Interestingly, flavonoid quercetin (QUE) has a strong antioxidant capacity [14-15] and has been observed to exhibit antibiofilm effects against several pathogenic Gram-positive and negative bacteria such as *Staphylococcus aureus*, *Staphylococcus epidermidis*, *Pseudomonas aeruginosa*, *Salmonella enterica*, and *Salmonella typhimurium* [16-21]. Quercetin was observed able to inhibit these bacteria's quorum sensing [16-20], virulence factors [16-17, 20], and biofilm formation ([16, 18-21]. Most importantly, quercetin provides cytoprotective effects to the host cells during bacterial infection [17] and does not impair bacterial growth which may lead to drug resistance [19].

Multi-walled carbon nanotubes (MWCNTs) which represent several layers of graphite [22] have been incorporated with chitosan-based membranes and hydrogels for several reasons including increased mechanical strength ([23], provide photothermal ability [24] and antibacterial activity [25]. Although MWCNTs pose unique properties that attract their use for biomedical purposes, studies have shown that pristine untreated CNTs that lack of any hydrophilic functional group are hardly dispersed in water, tend to aggregate and precipitate in aqueous solutions as well as impose toxicity at cellular and organ levels [22-26]. Therefore, functionalization of CNTs must be done to solve the problems with dispersion and toxicity, either covalently or noncovalently, by treatment with acids, surfactants or other agents to add polar functional groups to their structure [22, 26]. An earlier study by Kittana and colleagues [22] demonstrated that wounds treated with 5% chitosan-MWCNTs (acid-treated) hydrogel resulted in drier, better closed and smaller size wounds compared to treatment with pure chitosan hydrogel and 1% chitosan-MWCNTs. The study also pointed out that the chitosan-CNTs hydrogels are biocompatible, promote the synthesis of connective tissue by fibroblast cells, and improve the re-epithelialization of wounds. However, the investigators noticed that chitosan-MWCNTs with 5% MWCNTs resulted in more fibrosis following the deposition of large amounts of collagen by fibroblasts.

Regardless of the different types of modern wound dressings available, some limitations still exist considering the different etiologies and pathologies of healing each chronic wound has [9]. It is noteworthy that ideal wound dressings should provide a moist environment, promote epidermal migration and enzyme accumulation as well as enhance connective tissue synthesis and angiogenesis [27-28]. Although the moist environment is critical to trigger re-epithelialization and

granulation processes, it must be strictly regulated to avoid the wound fluid plays a role as a wounding agent. The wound with excess hydration can develop wound maceration especially in the presence of elevated matrix metalloproteinases, leading to chronic wounds [29]. The ideal wound dressings must also be non-adherent, sterile, non-toxic, permit debridement activity and gas exchange as well as have analgesic and antibacterial [27-28]. This study aims to synthesize a wound dressing comprises of chitosan biopolymer, MWCNTs, and quercetin in the form of a membrane and to evaluate the physicochemical properties of developed MWCNT/QUE/CS blended membrane. Comparison with pure CS membrane was conducted in terms of surface morphology, elemental and structural compositions, wettability, water absorption as well as water vapor transmission rate (WVTR). The blend of these three materials in the form of membrane may provide better membrane properties than pure CS membrane and the difference between the two membranes was investigated in this study.

Materials and Methods

Materials

Chitosan (medium molecular weight, 75-85% deacetylated), quercetin ($C_{15}H_{10}O_7$) and sodium hydroxide (NaOH) were supplied by Sigma-Aldrich, Germany. Multi-walled carbon nanotubes (MWCNTs) powder was purchased from local supplier. Glacial acetic acid (CH_3COOH) was supplied by J.T. Baker, Thailand and methanol (CH_3OH) were purchased from QReC, Malaysia.

Synthesis of Chitosan Membranes

Pure CS membrane synthesis was performed according to [30], with modifications. Initially, 0.7 g of chitosan powder was dissolved in 70 mL of 1% (v/v) acetic acid. This CS solution was stirred for 24 h at 50 °C. Once fully dissolved, the CS solution was sonicated and left for 15 min at room temperature to allow air bubbles to disappear before being poured into petri dishes (diameter of 85 mm) at a final volume of 30 mL. To facilitate complete solvent evaporation, the petri dish was oven-dried at a constant temperature of 50 °C for 48 h. The dried CS membrane was later neutralized in 10% (w/v) NaOH for 45 min, soaked and rinsed several times with distilled water before dried again at room temperature for 24 h. The CS membranes were synthesized in triplicates.

Synthesis of MWCNT/QUE/CS Blended Membranes

MWCNT/QUE/CS blended membranes were prepared by mixing chitosan-acetic acid solution, quercetin-methanol solution, and multi-walled carbon nanotubes-acetic acid solution with ratio 1:1:3. Specifically, 0.42 g of chitosan powder was dissolved in 42 mL 1% (v/v) acetic acid to form a CS solution. 0.14 g of QUE and MWCNTs were dissolved in methanol and 1% (v/v) acetic acid, respectively. The QUE and MWCNTs solutions were added into the CS solution and stirred at 50 °C for 24 h to obtain MWCNT/QUE/CS solution. The remaining steps were in accordance to the preparation of chitosan membranes. The MWCNT/QUE/CS blended membranes were prepared in triplicates.

Surface Morphology and Elemental Composition

The surface morphology of the CS and MWCNT/QUE/CS membranes was observed using a tabletop scanning electron microscope (TM3000, Hitachi, USA). This instrument was operated at the accelerating voltage of 15 kV and magnification of 100x to 1000x. Elemental composition identification and quantification of carbon, nitrogen and oxygen of the captured images were done using energy dispersive X-ray spectroscopy (EDX).

Structural Composition

The functional groups of both CS and MWCNT/QUE/CS membranes were analyzed using a fourier transform infrared spectroscopy (FTIR) coupled with an attenuated total reflection device (ATR) (IRTracer-100, Shimadzu Scientific Instruments, USA). The scanning range for the FTIR spectra was 4000-400 cm^{-1} at a resolution of 4 cm^{-1}.

Wettability

Evaluation of hydrophobic/hydrophilic property of CS and MWCNT/QUE/CS membranes was carried out using a video contact angle measurement machine (VCA Optima, AST Products, USA). 2 µL of water was dropped onto the membrane surface and three measurements of contact angle taken at different positions were recorded for each membrane.

Water Vapor Transmission Rate

The water vapor transmission rate (WVTR) of CS and MWCNT/QUE/CS membranes was determined gravimetrically according to the method of [31], with modifications. The membranes were cut into 15 mm x 15 mm and tightly sealed the 25 mL volumetric flask opening filled with 10 mL distilled water. The membrane area exposed to water vapor transmission was 0.79 cm^2. This volumetric flask was then weighed and placed in a desiccator containing dried silica gel kept at room temperature. The change in the weight of the volumetric flask was recorded at an interval of 24 h for 3 days and a graph of water loss versus time was plotted. The water vapor transmission rate of the membrane was calculated based on the following formula:

$$WVTR\ (g\ m^{-2}day^{-1}) = (W_t - W_o)\ /(tA)$$

Where W_o = weight of the initial system; W_t = weight of the system at time t; t = measurement time; A = open area of volumetric flask (m^2).

Swelling

This experiment was performed as previously described with some modifications [32]. The CS and MWCNT/QUE/CS membranes were first cut in a rectangular shape of 1 cm x 1 cm, weighed and recorded (W_0). The membrane cut was immersed in distilled water at room temperature for 1 h. The membrane was removed from distilled water at every 10 minute time intervals and blotted gently onto filter paper and immediately weighed (W_t). The soaking and weighing steps were repeatedly done for 1 h. The degree of swelling for each membrane was calculated using the following formula:

$$\text{Swelling ratio } [\%] = [W_0 - W_t] / W_0 \times 100$$

Where W_0 = Initial weight of membrane; W_t = Final weight of membrane after a particular soaking time, t.

Data analysis

All experiments were repeated at least three times. All data were expressed as mean ± standard deviation.

Results

Scanning electron microscopy was performed to compare the surface morphology of each membrane (Figure 1). The CS membrane surface was flat, compact and smooth, with the presence of impurities (Figures 1a-1b). The MWCNT/QUE/CS blended membrane showed uneven surface morphology, studded with dense granule-like structure as shown in Figures 1c-1d.

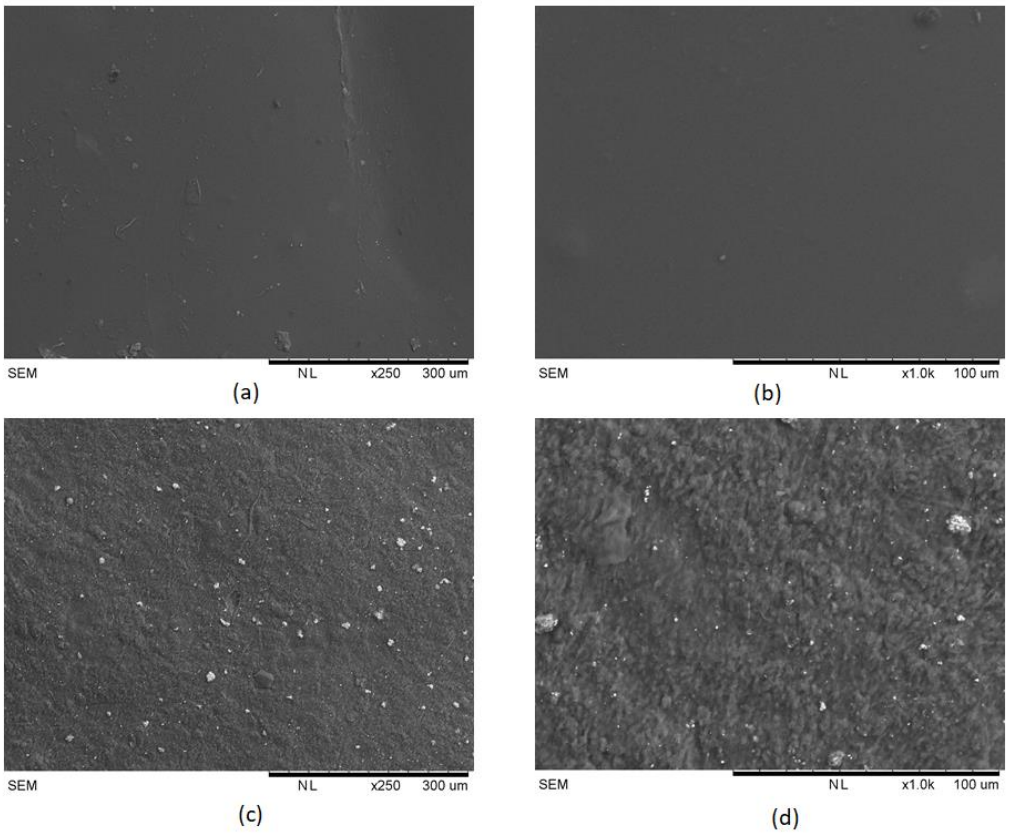

Figure 1. Surface morphology of: (a,b) CS and (c,d) MWCNT/QUE/CS membranes at 250x and 1000x magnifications, respectively

Table 1 depicts the elemental composition of carbon, nitrogen, and oxygen detected in CS and MWCNT/QUE/CS membranes using energy dispersive X-ray spectroscopy. The weight percentage of C in CS membranes (38.7%) was slightly higher than in the MWCNT/QUE/CS blended membranes (37.4%) (Table 1). However, the weight percentages of O and N were slightly lower in CS membranes than in the MWCNT/QUE/CS blended membranes.

Table 1. Elemental composition of CS and MWCNT/QUE/CS membranes.

Sample	Element (Atomic %), mean ± SD		
	C	O	N
CS	38.7 ± 3.3	32.8 ± 1.7	28.5 ± 2.0
MWCNT/QUE/CS	37.4 ± 2.6	33.4 ± 4.9	29.3 ± 4.7

Carbon (C), chitosan (CS), multi-walled carbon nanotubes (MWCNTs), nitrogen (N), oxygen (O), quercetin (QUE), standard deviation (SD).

Figure 2 indicates the FT-IR spectra of CS and MWCNT/QUE/CS membranes. The pure CS membrane showed strong and broad bands around 3000-3600 cm^{-1} which refer to the stretching vibration of –OH and –NH groups as well as inter chains hydrogen bonding of the polysaccharide. In this region, the two bands at 3290.56 and 3342.64 cm^{-1} corresponded to the primary amine group stretching vibration [33]. The chitosan spectrum at 2875.86 cm^{-1} corresponded to the –CH stretching vibration [34-35]. The band at 1649.14 cm^{-1} was assigned to –C=O stretching vibration of amide I [35-36] whereas the band at 1560.41 cm^{-1} refers to amide II N-H stretching [35, 37-38]. The band at 1600 cm^{-1} assigned to NH_2 deforming vibration overlapped with the amide I band at 1649.14 cm^{-1} giving a strong peak [33]. The C-N stretching vibration of amide III was found at 1317.38 cm^{-1} [36]. The band at 1149.57 cm^{-1} was the characteristic of asymmetric stretching vibration of the saccharide

structure of chitosan (C-O-C bridge) [36-37, 39]. The band at 1024.20 cm^{-1} was assigned to the –C-O stretch of C_6-OH groups of chitosan [34, 36]. Band at 894.97 cm^{-1} also corresponded to the saccharide structure [33].

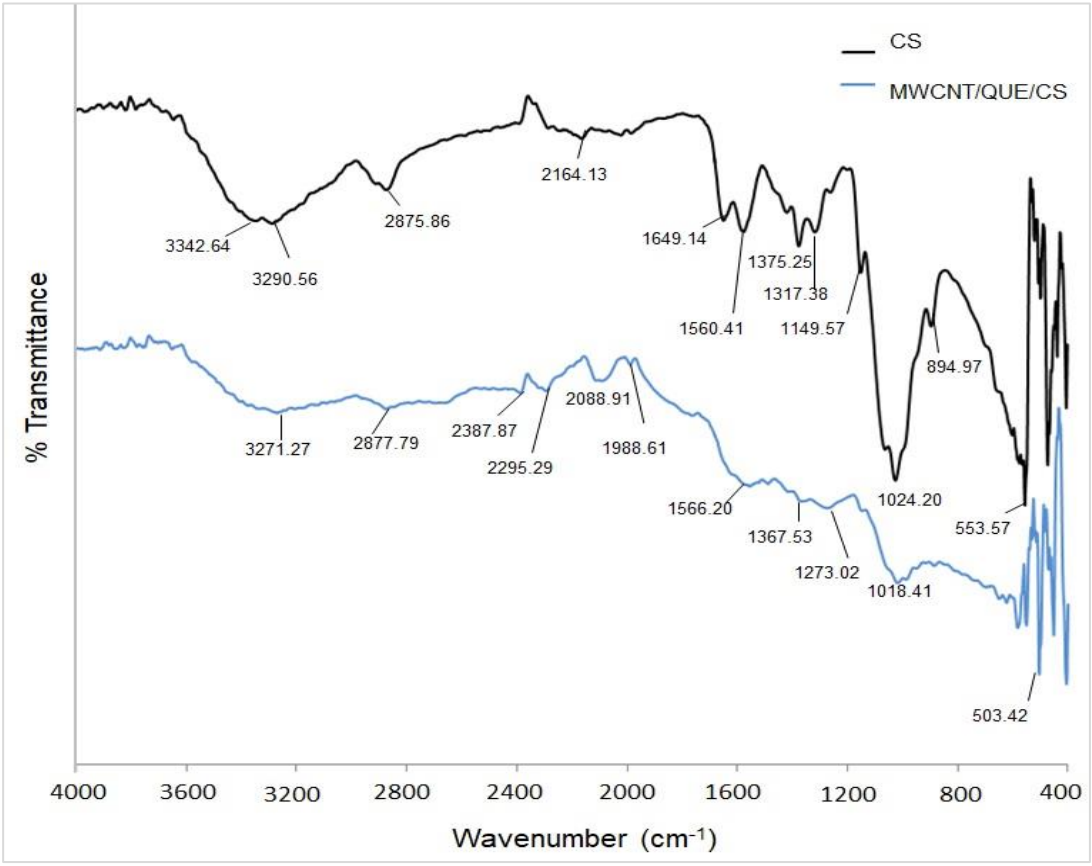

Figure 2. FTIR spectra of CS and MWCNT/QUE/CS membranes

In comparison, the FTIR spectrum of the MWCNT/QUE/CS blended membrane showed a broad absorption peak around 3271.27 cm^{-1} attributes to overlapping of –OH and –NH stretching vibrations [40] (Figure 2). Weak absorption bands of –CH symmetric stretching vibration and –C-O stretching were shown at 2877.79 cm^{-1} and 1018.41 cm^{-1}, respectively. The absorption band assigned to –C=O stretching vibration of amide I at 1649.14 cm^{-1} as shown in pure CS membrane was not observed in the MWCNT/QUE/CS blended membrane. A shifted and decrease in intensity of amide II band was observed at 1566.20 cm^{-1}. Specific bands corresponding to flavonoid quercetin –CH2- bending and –C-O stretching vibration were shown at 1367.53 cm^{-1} and 1273.02 cm^{-1}, respectively [41-42]. Two new bands were observed at 2088.91 cm^{-1} and around 1700 – 1750 cm^{-1} which represent the characteristic of –C=O stretching of MWCNT for the latter [35-40].

The combination of MWCNTs and QUE within the CS polymer matrix at the ratio 1:1:3 decreases the water contact angle value. It can be seen from Table 2 that the water contact angle of CS and MWCNT/QUE/CS membranes differ greatly. The pure CS membrane showed a higher water contact angle of 81.4° than the MWCNT/QUE/CS membrane (64.7°).

Table 2. Water contact angle of CS and MWCNT/QUE/CS membranes.

Sample	Water contact angle (º), mean ± SD
CS	81.4 ± 2.2
MWCNT/QUE/CS	64.7 ± 3.7

Chitosan (CS), multi-walled carbon nanotubes (MWCNTs), quercetin (QUE), standard deviation (SD).

Figure 3 presents the water vapour transmission rate (WVTR) of CS and MWCNT/QUE/CS membranes. It can be observed that the WVTR of the CS membrane was higher than MWCNT/QUE/CS membrane measured for three consecutive days. The highest WVTR values of 19.2 and 16.3 g/m^2.day were obtained after 24 h of the experiment for CS and MWCNT/QUE/CS membranes, respectively.

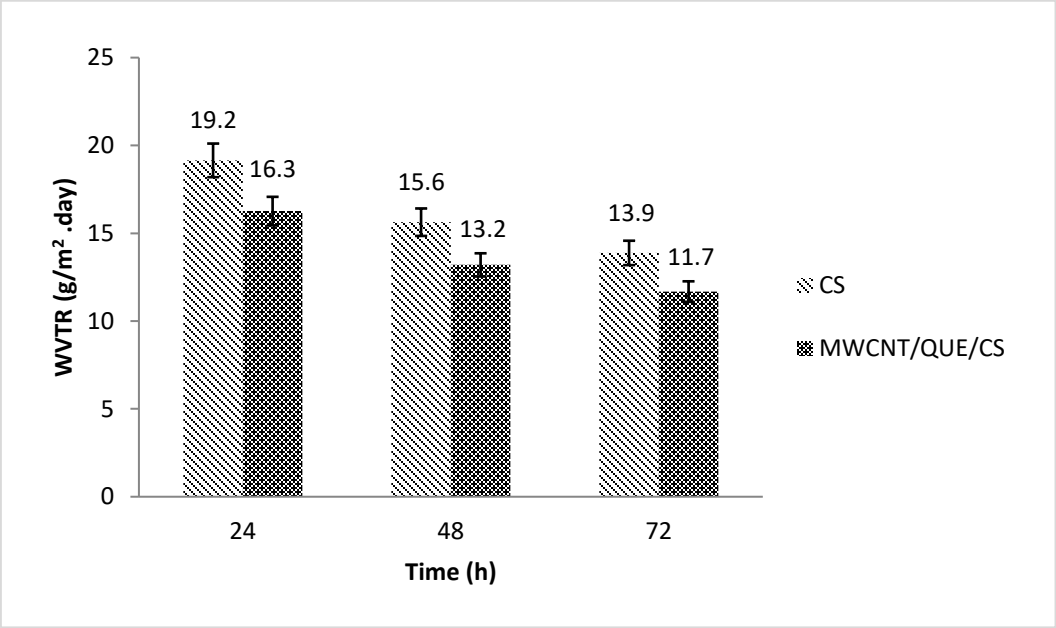

Figure 3. WVTR of CS and MWCNT/QUE/CS membranes

Results of water loss for both membranes were presented in Figure 4. The water loss achieved by the CS membrane was constant with an increment of 0.02 g per day as compared to the MWCNT/QUE/CS membrane which exhibited a decreasing trend of water loss as observed at 72 h of experiment (Figure 4).

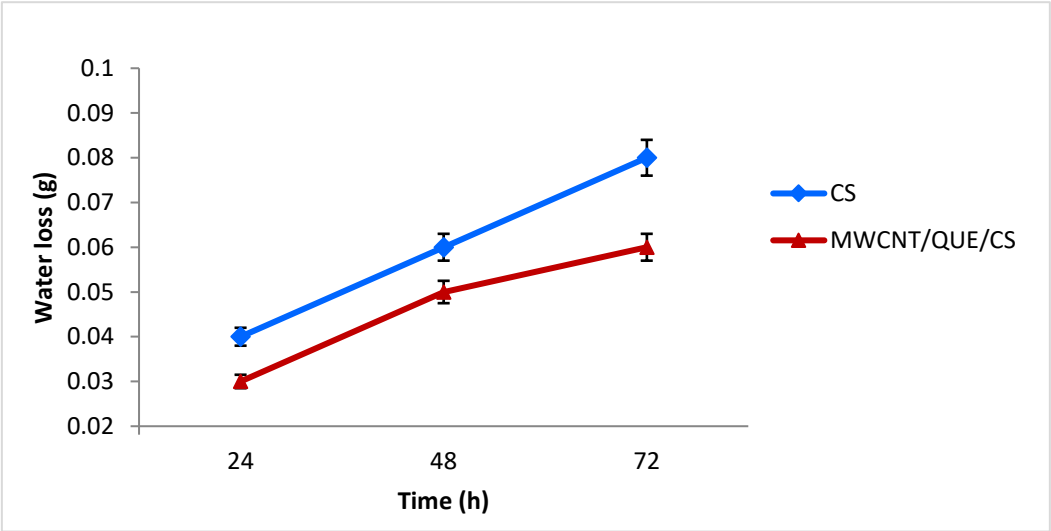

Figure 4. Water loss of CS and MWCNT/QUE/CS membranes

The swelling ratio of CS and MWCNT/QUE/CS membranes measured in 60 min was presented in Figure 5. The swelling ratio of MWCNT/QUE/CS membrane after 60 min was 90%, which is lower

than the CS membrane (105%). It can be observed that the CS membrane absorbed more water within the first ten minutes and reached saturation after 30 min than the MWCNT/QUE/CS membrane. The inclusion of quercetin into the CS matrix resulted in lower swelling index of the MWCNT/QUE/CS membrane. This can be explained by the hydrophobic nature of quercetin and hydrophobic or hydrogen bonding formation between quercetin and chitosan molecules [43].

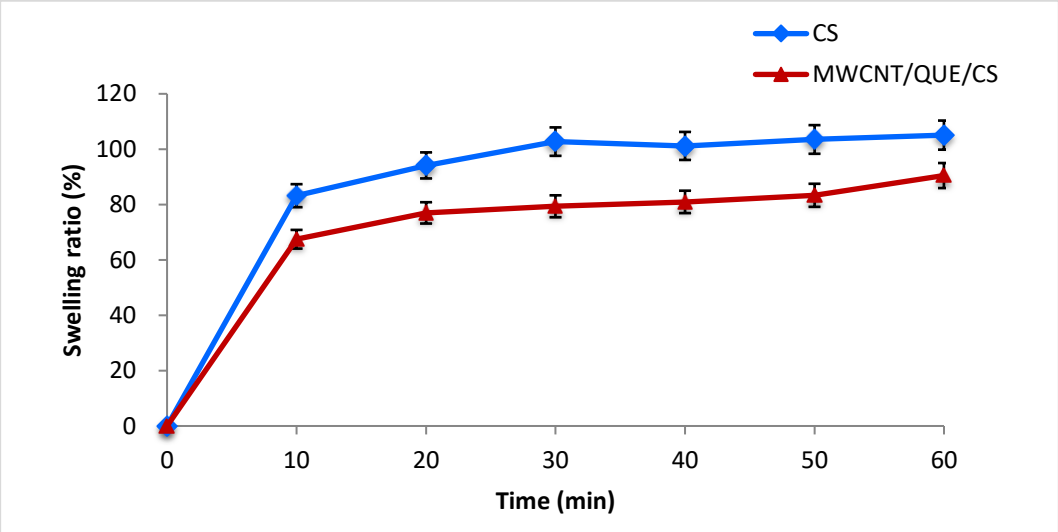

Figure 5. Swelling ratio of CS and MWCNT/QUE/CS membranes in 60 min

Discussions

The CS and MWCNT/QUE/CS membranes were prepared by stirring and ultrasonication. This technique allows the absorption of MWCNTs into the chitosan polymer matrix by electrostatic interaction and prevents aggregation [44]. The solvent casting technique provides several advantages for the synthesis of composite membranes including large area coverage, low temperature process ability, low cost and structural flexibility [26]. The MWCNTs used in this study were functionalized with 1% v/v acetic acid to reduce its toxicity and enhance its dispersion in aqueous environment [22, 26]. As a result, the acid functionalized MWCNTs contain hydrophilic groups such as –OH and –COOH [44].

Surface morphology results clearly presented a significant change in the surface morphology of CS and MWCNT/QUE/CS membranes. A similar observation has been reported for the CS film prepared using tartaric acid where impurities were observed at the surface of the CS film [45]). A smooth flat surface with an absence of pores was also observed for CS film prepared in acetic acid [30]. [31] also demonstrated that their CS film was homogenous and well-ordered, in comparison to the plant extract-chitosan composite film which showed uneven surface morphology. Similarly, it was observed in this study that the uneven surface of MWCNT/QUE/CS membrane could be attributed by the QUE. This phenolic compound is rich in a hydroxyl group, which may promote inter- and intramolecular hydrogen bonding with CS and result in uneven surface morphology of the MWCNT/QUE/CS membrane [31]. Though was not observed in this study, the presence of MWCNTs in MWCNT-CS composite films revealed that MWCNTs were coated with CS and appeared in a strand-like structure that would gather together at high MWCNTs content [46].

The C, O and N elements observed for both CS and MWCNT/QUE/CS membranes were contributed by the existence of N-acetyl D-glucosamine and D-glucosamine units in the chitosan structure [47]. The C and O elements were also derived from acid functionalized MWCNTs which were treated with acetic acid prior to the membrane formation, and quercetin. Slight changes in the elemental composition of chitosan were noticed following the addition of MWCNTs and quercetin at the ratio 1:1:3. Increase in O and N elements as seen for the MWCNT/QUE/CS membrane (Table 1) may indicate that more –OH and –NH functional groups are present on the membrane surface [48].

For the FTIR results (Figure 2), the disappearance of a doublet at 3342.64 and 3290.56 cm^{-1} in CS membrane as well as the appearance of a single, shifted band at 3271.27 cm^{-1} and narrowing of the wide band at 3000-3600 cm^{-1} in MWCNT/QUE/CS membrane indicating the partial destruction of superimposed –OH and amine –NH symmetrical stretching vibrations and the hydrogen bonding extensive formation, most likely due to the interaction of chitosan primary amine with –OH groups of quercetin and MWCNTs and hydroxyl group of chitosan with quercetin [39, 42]. The disappearance of the characteristic band at 1649.14 cm^{-1} was also observed in earlier studies [39, 42]. There are two possible explanations for this observation. First, this peak disappeared due to the shifting of the –C=O functional group following the intermolecular hydrogen bond interaction between MWCNTs and CS [44]. Second, the –NH group of chitosan interaction with the functional group of quercetin resulted in the peak disappearance [42]. The reaction between a carboxylic group of MWCNTs and amino groups of chitosan during the modification will form amide (-CONH-) groups around 1300-1650 cm^{-1} [44]. On the contrary, this study observed a shifted and lower intensity of the overall band at 1300-1650 cm^{-1} suggesting that the quercetin could have completely interacted with the CS matrix and MWCNTs [39, 42].

The water contact angle results as shown in Table 2 were influenced by the elemental composition of the membrane surface. The presence of more –OH and –NH groups on the MWCNT/QUE/CS membrane surface may increase this membrane surface hydrophilicity and decrease its water contact angle as a result of hydrogen bonds formation between chitosan, MWCNTs and quercetin [48]. Thus, a decrease in water contact angle was demonstrated upon the addition of acid functionalized MWCNTs and quercetin into the chitosan polymer matrix. Similar observations were also reported by a past study where the addition of single-walled carbon nanotubes (SWCNTs) and MWCNTs in the acetic acid-chitosan hydrogel gives them hydrophilic properties which are needed for effective skin contact as well as adequate dispersal in aqueous media [22]. Previous studies also pointed out that the incorporation of bioactive materials such as curcumin and plant extracts into the polymer matrix resulted in greater wound healing capability than the pure polymer itself [13].

The WVTR value of CS membrane was higher than MWCNT/QUE/CS membrane (Figure 3). Low WVTR as seen in MWCNT/QUE/CS membrane could be attributed by the addition of quercetin to the composite membrane. Previous studies also demonstrated that the addition of phenolic compounds such as protocatechuic acid [49] and plant extract [31] into the chitosan polymer matrix decreases the composite films water vapor permeability values due to their low water affinity as compared to pure chitosan films. The presence of a hydrophilic domain in pure chitosan membrane greatly influences its successive diffusive step [31]. On the contrary, the interaction of quercetin with –OH and $–NH_2$ groups in chitosan and the presence of bulky benzene rings in quercetin molecules could have obstructed the polymer network, thus reducing the chitosan affinity towards water vapour [31, 49]. In addition, another study highlighted that the incorporation of graphene oxide (GO) nanosheets into the polyvinyl alcohol polymer matrix resulted in resistance to water molecules penetration. This lowers the WVTR value due to a larger diffusion length and a longer diffusion time taken by water molecules as they avoid the GO nanosheets within the polymer matrix [50]. Thus, it can be deduced that the presence of MWCNTs may as well resist water molecules penetration and contribute to the low WVTR value of the MWCNT/QUE/CS membrane. For wound dressing application, the WVTR value indicates the membrane ability to control water loss and a suitable WVTR will provide a moist environment needed for optimum wound healing [51]. It is noteworthy that an extremely high and low WVTR should be avoided as this may lead to wound dehydration and accumulation of wound exudates, respectively [51]. It can be suggested from the findings in Figure 4 that MWCNT/QUE/CS membrane showed better ability to control water loss than the CS membrane.

The swelling property of a wound dressing represents its ability to resist wound exudate accumulation and subsequently helps to prevent inflammation during the wound healing process [47]. The incorporation of quercetin into chitosan polymer matrix limits the interactions between chitosan and water molecules and resulted in less swelling ratio (Figure 5). This could be due to the interactions between –OH groups in quercetin with the hydrophilic groups in chitosan that lead to less polar side-chain groups' exposure to water molecules [43, 49]. Similar observations were also reported for the chitosan composite films containing protocatechuic acid and quercetin-starch [43, 49]. The pure CS membrane, conversely, demonstrated a higher swelling ratio in accordance with the earlier study as a result of strong hydrogen bond interactions between its –OH and –NH groups and water molecules [49]. Past findings also revealed that the addition of small amount of MWCNTs into gelatin-chitosan matrix increases the film hydrophobicity and lowers the swelling ability. This could be the result of the shielding effects of MWCNTs that were irregularly distributed in the polymer matrix forming a well-developed three-dimensional network, thus preventing solvent diffusion into the polymer matrix [26]. From Figure 5, it can be seen that an abrupt swelling occurs in both CS and

MWCNT/QUE/CS membranes within 10 minutes of immersion in distilled water followed by controlled swelling. Similarly, a previous study has reported the same observations for the chitosan/pectin/zinc oxide films that contain different amounts of zinc oxide nanoparticles [47]. In that study, the films showed abrupt swelling followed by controlled swelling until they reached a maximum swelling equilibrium. In comparison to chitosan/pectin film, the chitosan/pectin/zinc oxide films absorbed less water and thus showed lesser swelling degree, presumably due to less porosity, small pore size and chelation of zinc oxide nanoparticles with the hydrophilic groups of the polymer network [47].

Conclusions

The incorporation of functionalized MWCNTs and quercetin highly influences the physicochemical properties of the MWCNT/QUE/CS blended composite membrane. The increase in surface hydrophilicity of the blended membrane may support skin contact. The improved surface structure as shown from the uneven surface morphology of the MWCNT/QUE/CS membrane may promote re-epithelialization. The low WVTR of the MWCNT/QUE/CS membrane may suggest that wound surface dehydration can be prevented but more studies must be conducted to confirm the influence of WVTR on cell migration and wound healing. The presence of quercetin as the bioactive material in this blended membrane may accelerate wound healing due to its antibacterial and antioxidant properties. Thus, it is suggested from these findings that MWCNT/QUE/CS blended composite membrane has suitable properties for wound dressing application and could be further explored.

Conflicts of interest

The authors declare that there is no conflict of interest regarding the publication of this paper.

Funding Statement

This work was financially supported by the Ministry of Higher Education Malaysia and Universiti Teknologi Malaysia under Research University grant with reference number R.J130000.2651.17J40. All authors express their appreciation to the School of Biomedical Engineering and Health Sciences, Faculty of Engineering, UTM for the provided equipment and technical assistance.

References

[1] Ghomi, E. R., Khalili, S., Khorasani, S. N., Neisiany, R. E., & Ramakrishna, S. (2019). Wound dressings: Current advances and future directions. *Journal of Applied Polymer Science*, *136*(27), 47738.

[2] Hadian, Y., Bagood, M. D., Dahle, S. E., Sood, A., & Isseroff, R. R. (2019). Interleukin-17: Potential target for chronic wounds. Mediators of Inflammation, *2019*, 1-10.

[3] Rousselle, P., Braye, F., & Dayan, G. (2019). Re-epithelialization of adult skin wounds: Cellular mechanisms and therapeutic strategies. Advanced Drug Delivery Reviews, *146*, 344-365.

[4] Raziyeva, K., Kim, Y., Zharkinbekov, Z., Kassymbek, K., Jimi, S., & Saparov, A. (2021). Immunology of acute and chronic wound healing. *Biomolecules*, *11*(5), 700.

[5] Schilrreff, P., & Alexiev, U. (2022). Chronic inflammation in non-healing skin wounds and promising natural bioactive compounds treatment. *International Journal of Molecular Sciences*, *23*(9), 4928.

[6] Alvarez Echazú, M. I., Olivetti, C. E., Anesini, C., Perez, C. J., Alvarez, G. S., & Desimone, M. F. (2017). Development and evaluation of thymol-chitosan hydrogels with antimicrobial-antioxidant activity for oral local delivery. *Materials Science and Engineering: C*, *81*, 588-596.

[7] Ostapska, H., Howell, P. L., & Sheppard, D. C. (2018). Deacetylated microbial biofilm exopolysaccharides: It pays to be positive. *PLoS Pathogens*, *14*(12), e1007411.

[8] Marmont, L. S., Whitfield, G. B., Rich, J. D., Yip, P., Giesbrecht, L. B., Stremick, C. A., Whitney, J. C., Parsek, M. R., Harrison, J. J., & Howell, P. L. (2017). PelA and PelB proteins form a modification and secretion complex essential for Pel polysaccharide-dependent biofilm formation in Pseudomonas aeruginosa. *Journal of Biological Chemistry*, 292(47), 19411-19422.

[9] Brumberg, V., Astrelina, T., Malivanova, T., & Samoilov, A. (2021). Modern wound dressings: hydrogel dressings. *Biomedicines*, *9*(9), 1235.
[10] Akhoondinasab, M.-R., Karimi, H., Sheikhizadeh, S., & Saberi, M. (2019). Reducing pain at split thickness donor sites with silicone dressing compared to petrolatum gauze dressing. *Annals of Burns and Fire Disasters, 32*(3), 210-215.
[11] Wang, Y.-W., Liu, C.-C., Cherng, J.-H., Lin, C.-S., Chang, S.-J., Hong, Z.-J., Liu, C.-C., Chiu, Y.-K., Hsu, S.-D., & Chang, H. (2019). Biological effects of chitosan-based dressing on hemostasis mechanism. *Polymers*, *11*, 1906.
[12] Adnan, S., Ranjha, N. M., Hanif, M., & Asghar, S. (2020). O-Carboxymethylated chitosan; A promising tool with in-vivo anti-inflammatory and analgesic properties in albino rats. *International Journal of Biological Macromolecules*, *156*, 531-536.
[13] Abbas, M., Arshad, M., Rafique, M. K., Altalhi, A. A., Saleh, D. I., Ayub, M. A., Sharif, S., Riaz, M., Alshawwa, S.Z., Masood, N., Nazir, A., & Iqbal, M. (2022). Chitosan-polyvinyl alcohol membranes with improved antibacterial properties contained Calotropis procera extract as a robust wound healing agent. *Arabian Journal of Chemistry*, *15*(5), 103766.
[14] [14] Ismail, N. I., Sornambikai, S., Kadir, M. R. A., Mahmood, N. H., Zulkifli, R. M., & Shahir, S. (2018). Evaluation of radical scavenging capacity of polyphenols found in natural Malaysian honeys by voltammetric techniques. *Electroanalysis*, *30*(12), 2939-2949.
[15] Kale, A., Pişkin, Ö., Baş, Y., Aydın, B. G., Can, M., Elmas, Ö., & Büyükuysal, Ç. (2018). Neuroprotective effects of quercetin on radiation-induced brain injury in rats. *Journal of Radiation Research, 59*(4), 404-410.
[16] Ouyang, J., Sun, F., Feng, W., Sun, Y., Qiu, X., Xiong, L., Liu, Y., & Chen, Y. (2016). Quercetin is an effective inhibitor of quorum sensing, biofilm formation and virulence factors in Pseudomonas aeruginosa. *Journal of Applied Microbiology*, *120*(4), 966-974.
[17] Vipin, C., Mujeeburahiman, M., Ashwini, P., Arun, A. B., & Rekha, P.-D. (2019). Anti-biofilm and cytoprotective activities of quercetin against Pseudomonas aeruginosa isolates. *Letters in Applied Microbiology, 68*(5), 464-471.
[18] Mu, Y., Zeng, H., & Chen, W. (2021). Quercetin inhibits biofilm formation by decreasing the production of EPS and altering the composition of EPS in Staphylococcus epidermidis. *Frontiers in Microbiology*, *12*, 1-8.
[19] Kang, X., Ma, Q., Wang, G., Li, N., Mao, Y., Wang, X., Wang, Y., & Wang, G. (2022). Potential mechanisms of quercetin influence the ClfB protein during biofilm formation of Staphylococcus aureus. *Frontiers in Pharmacology*, *13*, 1-12.
[20] Kim, Y. K., Roy, P. K., Ashrafudoulla, M., Nahar, S., Toushik, S. H., Hossain, M. I., Mizan, M. F. R., Park, S. H., & Ha, S.-D. (2022). Antibiofilm effects of quercetin against Salmonella enterica biofilm formation and virulence, stress response, and quorum-sensing gene expression. *Food Control*, *137*, 108964.
[21] Roy, P. K., Song, M. G., & Park, S. Y. (2022). Impact of quercetin against Salmonella typhimurium biofilm formation on food–contact surfaces and molecular mechanism pattern. *Foods, 11*, 977.
[22] Kittana, N., Assali, M., Abu-Rass, H., Lutz, S., Hindawi, R., Ghannam, L., Zakarneh, M., & Mousa, A. (2018). Enhancement of wound healing by single-wall/multi-wall carbon nanotubes complexed with chitosan. *International Journal of Nanomedicine*, *13*, 7195-7206.
[23] Khoerunnisa, F., Rahmah, W., Seng Ooi, B., Dwihermiati, E., Nashrah, N., Fatimah, S., Ko, Y. G., & Ng, E.-P. (2020). Chitosan/PEG/MWCNT/Iodine composite membrane with enhanced antibacterial properties for dye wastewater treatment. *Journal of Environmental Chemical Engineering*, *8*(2), 103686.
[24] Liang, Y., Zhao, X., Hu, T., Han, Y., & Guo, B. (2019). Mussel-inspired, antibacterial, conductive, antioxidant, injectable composite hydrogel wound dressing to promote the regeneration of infected skin. *Journal of Colloid and Interface Science*, *556*, 514-528.
[25] [25] Abo-Neima, S. E., Motaweh, H. A., & Elsehly, E. M. (2020). Antimicrobial activity of functionalised carbon nanotubes against pathogenic microorganisms. *IET Nanobiotechnology*, *14*(6), 457-464.
[26] Sharmeen, S., Rahman, A. F. M. M., Lubna, M. M., Salem, K. S., Islam, R., & Khan, M. A. (2018). Polyethylene glycol functionalized carbon nanotubes/gelatin-chitosan nanocomposite: An approach for significant drug release. *Bioactive Materials*, *3*(3), 236-244.
[27] [27] Jahromi, M. A. M., Zangabad, P. S., Basri, S. M. M., Zangabad, K. S., Ghamarypoure, A., Aref, A. R., Karimi, M., & Hamblin, M. R. (2018). Nanomedicine and advanced technologies for burns: Preventing infection and facilitating wound healing. *Advanced Drug Delivery Reviews*, *123*, 33-64.
[28] Ambekar, R. S., & Kandasubramanian, B. (2019). Advancements in nanofibers for wound dressing: A review. *European Polymer Journal*, *117*, 304-336.

[29] Crowe, E., Scott, C., Cameron, S., Cundell, J. H., & Davis, J. (2022). Developing wound moisture sensors: opportunities and challenges for laser-induced graphene-based materials. *Journal of Composites Science, 6*(6), 176.
[30] Fideles, T. B., Santos, J. L., Tomás, H., Furtado, G. T. F. S., Lima, D. B., Borges, S. M. P., & Fook, M. V. L. (2018). Characterization of chitosan membranes crosslinked by sulfuric acid. *Open Access Library Journal*, *5*, e4336.
[31] Kadam, D., & Lele, S. S. (2018). Cross-linking effect of polyphenolic extracts of Lepidium sativum seedcake on physicochemical properties of chitosan films. *International Journal of Biological Macromolecules*, *114*, 1240-1247.
[32] Vedakumari, W. S., Ayaz, N., Karthick, A. S., Senthil, R., & Sastry, T. P. (2017). Quercetin impregnated chitosan–fibrin composite scaffolds as potential wound dressing materials — Fabrication, characterization and in vivo analysis. *European Journal of Pharmaceutical Sciences*, *97*, 106-112.
[33] Mohamed, N. A., & Abd El-Ghany, N. A. (2019). Synthesis, characterization and antimicrobial activity of novel aminosalicylhydrazide cross linked chitosan modified with multi-walled carbon nanotubes. *Cellulose*, *26*(2), 1141-1156.
[34] Wang, X., Tang, R., Zhang, Y., Yu, Z., & Qi, C. (2016). Preparation of a novel chitosan based biopolymer dye and application in wood dyeing. *Polymers*, *8*, 338.
[35] Malekkiani, M., Magham, A. H. J., Ravari, F., & Dadmehr, M. (2022). Facile fabrication of ternary MWCNTs/ZnO/Chitosan nanocomposite for enhanced photocatalytic degradation of methylene blue and antibacterial activity. *Scientific Reports*, *12*, 5927.
[36] Diao, Y., Yu, X., Zhang, C., & Jing, Y. (2020). Quercetin-grafted chitosan prepared by free radical grafting: characterization and evaluation of antioxidant and antibacterial properties. *Journal of Food Science and Technology*, *57*(6), 2259-2268.
[37] Nataraj, D., Sakkara, S., Meghwal, M., & Reddy, N. (2018). Crosslinked chitosan films with controllable properties for commercial applications. *International Journal of Biological Macromolecules*, *120*, 1256-1264.
[38] Cheng, J., Zhu, H., Huang, J., Zhao, J., Yan, B., Ma, S., Zhang, H., & Fan, D. (2020). The physicochemical properties of chitosan prepared by microwave heating. *Food Science & Nutrition, 8*, 1987-1994.
[39] Francis, A. A., Abdel-Gawad, S. A., & Shoeib, M. A. (2021). Toward CNT-reinforced chitosan-based ceramic composite coatings on biodegradable magnesium for surgical implants. *Journal of Coatings Technology and Research*, *18(*4), 971-988.
[40] Metwally, N. H., Saad, G. R., & Abd El-Wahab, E. A. (2019). Grafting of multiwalled carbon nanotubes with pyrazole derivatives: Characterization, antimicrobial activity and molecular docking study. *International Journal of Nanomedicine*, *14*, 6645-6659.
[41] Porto, I. C. C. M., Nascimento, T. G., Oliveira, J. M. S., Freitas, P. H., Haimeur, A., & França, R. (2018). Use of polyphenols as a strategy to prevent bond degradation in the dentin-resin interface. *European Journal of Oral Sciences*, *126*, 1-13.
[42] Stanicka, K., Dobrucka, R., Woźniak, M., Sip, A., Majka, J., Kozak, W., & Ratajczak, I. (2021). The effect of chitosan type on biological and physicochemical properties of films with propolis extract. *Polymers*, *13*, 3888.
[43] Yadav, S., Mehrotra, G. K., Bhartiya, P., Singh, A., & Dutta, P. K. (2020). Preparation, physicochemical and biological evaluation of quercetin based chitosan-gelatin film for food packaging. *Carbohydrate Polymers*, *227*, 115348.
[44] Thou, C. Z., Khan, F. S. A., Mubarak, N. M., Ahmad, A., Khalid, M., Jagadish, P., Walvekar, R., Abdullah, E. C., Khan, S., Khan, M., Hussain, S., Ahmad, I., & Algarni, T. S. (2021). Surface charge on chitosan/cellulose nanowhiskers composite via functionalized and untreated carbon nanotube. *Arabian Journal of Chemistry*, *14*, 103022.
[45] Cui, L., Gao, S., Song, X., Huang, L., Dong, H., Liu, J., Chen, F., & Yu, S. (2018). Preparation and characterization of chitosan membranes. *RSC Advances*, *8*(50), 28433–28439.
[46] Qi, P., Xu, Z., Zhang, T., Fei, T., & Wang, R. (2020). Chitosan wrapped multiwalled carbon nanotubes as quartz crystal microbalance sensing material for humidity detection. *Journal of Colloid and Interface Science*, *560*, 284-292.
[47] Soubhagya, A. S., Moorthi, A., & Prabaharan, M. (2020). Preparation and characterization of chitosan/pectin/ZnO porous films for wound healing. *International Journal of Biological Macromolecules, 157*, 135-145.
48] Ganji, P., Nazari, S., Zinatizadeh, A. A., & Zinadini, S. (2022). Chitosan-wrapped multi-walled carbon nanotubes (CS/MWCNT) as nanofillers incorporated into nanofiltration (NF) membranes aiming at remarkable water purification. *Journal of Water Process Engineering*, *48*, 102922.
[49] Liu, J., Liu, S., Wu, Q., Gu, Y., Kan, J., & Jin, C. (2017). Effect of protocatechuic acid incorporation on the physical, mechanical, structural and antioxidant properties of chitosan film. *Food Hydrocolloids, 73*, 90-100.

[50] Fan, J., Zhou, W., Wang, Q., Chu, Z., Yang, L., Yang, L., Sun, J., Zhao, L., Xu, J., Liang, Y., & Chen, Z. (2018). Structure dependence of water vapor permeation in polymer nanocomposite membranes investigated by positron annihilation lifetime spectroscopy. *Journal of Membrane Science*, *549*, 581-587.

[51] Xu, R., Xia, H., He, W., Li, Z., Zhao, J., Liu, B., Wang, Y., Lei, Q., Kong, Y., Bai, Y., Yao, Z., Yan, R., Li, H., Zhan, R., Yang, S., Luo, G., & Wu, J. (2016). Controlled water vapor transmission rate promotes wound-healing via wound re-epithelialization and contraction enhancement. *Scientific Reports*, *6*, 24596.